OPTOELECTRONICS AND ADVANCED MATERIALS – RAPID COMMUNICATIONS Vol. 3, No. 9, September 2009, p. 899 - 903

Innovating transparent glass ceramics based on $Ga_2S_3 – GeS_2 – CsCl$

Y. LEDEMI[a,c*], B. BUREAU[a], L. CALVEZ[a], M. ROZE[a], E. GUILLEVIC[a], N. AUDEBRAND[b], M. POULAIN[a], Y. MESSADDEQ[c], X.H. ZHANG[a]

[a]*Equipe Verres et Céramiques, UMR 6226 Sciences Chimiques de Rennes, Université de Rennes 1, Campus de Beaulieu, 35042 Rennes, France*

[b]*Equipe Matériaux inorganiques: Chimie douce et réactivité, UMR 6226 Sciences Chimiques de Rennes, Université de Rennes 1, Campus de Beaulieu, 35042 Rennes, France*

[c]*Laboratorio dos Materiais Fotônicos, Instituto de Química, Universidade Estadual Paulista, 14801-970 Araraquara/SP, Brazil*

In this paper, we describe the preparation of glass ceramics in the $Ga_2S_3 – GeS_2 – CsCl$ system. Visible and infrared transmitting glass ceramics were reproducibly obtained by appropriated heat treatment of the base glass. Crystals with controllable size of about 40 nm were homogeneously generated in the glassy matrix. X-ray diffraction characterizations have shown that gallium acts as nucleating agent in this material, giving rise to α-Ga_2S_3 crystals. Improved thermo-mechanical properties such as dilatation coefficient and resistance to fracture propagation have been observed in the prepared glass ceramics.

(Received December 27, 2008; accepted September 15, 2009)

Keywords: Chalco halides, Crystallization, Glass-ceramics, Infrared glasses

1. Introduction

Chalcogenide glasses (based on chalcogen elements: S, Se and Te) have been intensively studied for a long time for their unique properties: low phonon energies, high refractive indices, extended transparency in the infrared spectral range and photosensibility [1-5]. They can be easily shaped by molding or drawn into fibers [6, 7], leading to various potential applications such as lenses for thermal imaging [8], optical fibers for chemical or biological sensing [9-11], waveguides for space [12, 13] or optical data storage [14].

Nevertheless, many applications that chalcogenide glasses offer can be limited by their relatively weak mechanical properties. A well known route to improve the mechanical properties of a glass, as its toughness - resistance to fracture propagation - or resistance to thermal shocks, is to generate crystals inside the glassy matrix. Recently, infrared transparent glass ceramics based on chalcohalide have been obtained [15]. It has been demonstrated that the addition of alkali halide such as cesium chloride into the glass matrix leads to a better control of the ceramization process, avoiding too fast and uncontrollable growth of crystals inside the material.

Previous works have shown the feasibility of preparing reproducible transparent glass ceramics in the $GeSe_2 – Sb_2Se_3 – MX$ system (M: Cs, Rb; X: Cl, I) [16, 17] as well as in the sulphide equivalent system [18; 19]. Furthermore, glass ceramics transmitting from the visible range to the far infrared were also obtained in the $Ga_2Se_3 – GeSe_2 – CsCl$ system [20] [20].

Another potential application of chalcogenide glass ceramic is the generation of crystalline low phonon energy environment around rare earth ions [21] which can lead to higher quantum efficiency. Moreover it has been established that introduction of rare earth ions in germanium sulphide based glasses is easier in presence of gallium sulphide. So the $Ga_2S_3 – GeS_2 – CsCl$ system appears as a good candidate for rare earth ions doping.

In this paper, the preparation of transparent glass ceramics in the $Ga_2S_3 – GeS_2 – CsCl$ system has been reported. X-ray diffraction and Scanning Electron Microscopy (SEM) have been used to characterize the prepared glass ceramics. Optical and thermo-mechanical properties of the prepared materials are also presented hereby.

2. Experimental details

The Ga_2S_3-GeS_2-CsCl glasses were synthesized using highly pure polycrystalline germanium (5N), gallium (5N), sulphur (5N) and cesium chloride (3N). More details about the preparation of samples are given in a previous work [22] [22]. The typical batch size was 10 g, leading to a glass rod of 10 mm diameter and 50 mm length. The glass rods were then sliced into discs of 2 mm thick and polished. In a first step heat treatments have been

performed on the glass discs in a ventilated furnace at different temperatures with an accuracy of +/- 2°C in order to determine the optimal ceramization temperature. Finally glass ceramics have been heat treated for different durations at the most suitable temperature. It is important to notice that glass ceramics were reproducibly obtained from different glass rods following this process.

Optical transmission was measured using a CARY5 double beam spectrophotometer (Varian) for the visible and near infrared region while a FTIR VECTOR 22 spectrophotometer (Bruker) was used for the mid and far infrared region.

To observe submicron crystals under scanning electronic microscope, samples were coated with a very thin gold palladium layer because of the electrical insulator character of chalcogenide glasses. Then, small cracks were created on the glass surface in order to observe inside the glass ceramics and also to eliminate the gold coating influence.

Thermal analysis experiments were performed using a differential scanning calorimeter DSC 2910 (TA Instruments) from room temperature to 550°C (to avoid the apparatus deterioration) with a heating rate of 10°C/min. Dilatation experiments were carried out on a TMA 2940 Calorimeter (TA Instruments). Polished samples with a thickness of 4 to 6 mm were heated at 2°C/min up to the glass transition temperature, the thermal expansion coefficient α (K^{-1}) was measured between 100 and 250°C.

For X-ray diffraction measurements, samples were firstly crushed in fine powder. Data were then collected using a Bragg – Brentano Siemens D500 diffractometer equipped with a primary-beam germanium monochromator (Cu $K\alpha_1$) with a step of 0.02° and a counting time of 12s per step.

Mechanical properties such as Hardness (Hv) and toughness (Kc) were determined using a Vickers micro indenter with a charge of 100g during 5s.

3. Results and discussion

3.1 Glass-ceramics preparation

The glass forming ability of the $Ga_2S_3 – GeS_2 – CsCl$ pseudo ternary system was firstly reported by Tver'yanovitch et al. [26]. In a previous work, the optical and thermal properties of glasses belonging to this system have been studied in function of the CsCl content [22]. It was shown that very large amount of alkali halide can be incorporated into the $Ga_2S_3 – GeS_2$ glasses. However, because of the hygroscopic character of the CsCl ionic compound, glasses with high CsCl content present a weaker resistance to moisture. In order to minimize this effect, a low CsCl content glass composition - $(Ga_2S_3)_{25} – (GeS_2)_{65} – (CsCl)_{10}$ -was chosen for this study.

The glass transition temperature of the base glass, determined by DSC, is Tg = 405°C. A systematic isothermal treatment of the glass performed at different temperatures above Tg has shown that T = 425°C is the more appropriated temperature to control the nucleation and growth of crystals inside the glassy matrix. Thus, a series of glass ceramics has been prepared by heat treatment at 425°C with different durations varying from 2h up to 65h. For a better readability, the base glass will be named GC0 and the prepared glass ceramics will be labelled GCx, with x the annealing time (h).

As it can be seen in Fig. 1, crystals are homogeneously generated inside the glassy matrix. Furthermore, a simple observation with the naked eye shows a progressive opacity of the glass ceramics in the visible range with increasing heat treatment time. One can also observe a bleaching colour of the glass ceramic after 65h of ceramization.

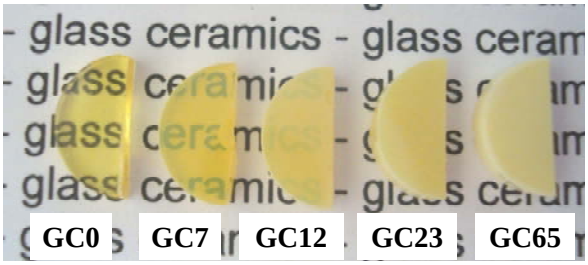

Fig. 1. Photography of the base glass and glass ceramics for different heat treatment times.

3.2 Optical properties

The optical transmission spectrum of the glass ceramics are presented in Fig. 2. It can be seen in Fig. 2 (a) that the beginning of transmission in the visible region is shifted toward longer wavelength with increasing annealing time. Significant scattering losses are observed after 7h of ceramization; for longer durations (23h) the glass ceramics become totally opaque in the visible range. Fig. 2 (b) presents the transmission measured in the infrared region. Glass ceramics treated up to 23h maintain a good infrared transmission. For a heat treatment time of 36h, the transmission starts to fall drastically and for longer time of annealing (x > 36h) the material becomes totally opaque in the infrared window. The absorption bands observed at 2.9, 4.1 and 6.3 µm are respectively due to OH, SH and H_2O impurities. The heat treatments performed in ambient atmosphere can explain the increasing absorption bands due to moisture.

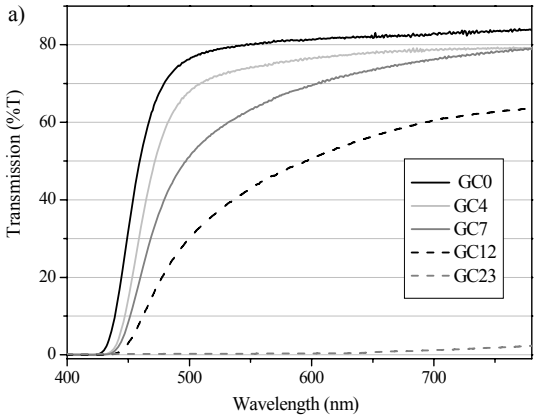

(a)

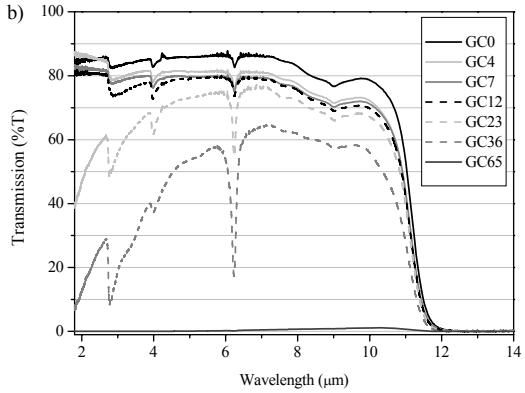

(b)

Fig. 2. Optical transmission spectra of GCx samples (a) in the visible region and (b) in the infrared region.

Scanning electronic micrograph of glass ceramics GC7 (a) and GC23 (b) are shown in Fig. 3. In the GC7 sample, the crystals (white spots) are uniformly distributed and the size distribution is homogeneous with an average diameter of about 40 nm. For the GC23 sample, which is totally opaque in the visible range, crystals are much bigger, but their dimensions remain below the micron, the crystallized fraction volume, estimated from SEM pictures, is higher than 50 % and the crystals seem relatively interconnected. It is important to notice that GC23 sample is still transparent in the infrared region, as it was shown in Fig. 2.

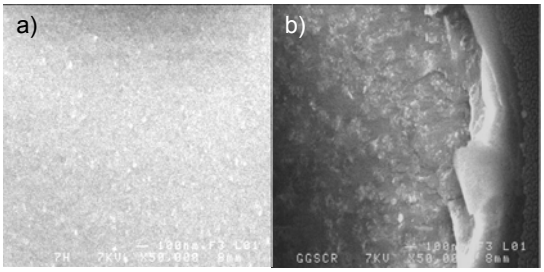

Fig. 3. SEM micrograph of GC7 (a) and GC23 (b) samples.

3.3 Thermal analysis

Thermal analysis experiments were performed on the glass ceramics. The obtained DSC curves have been reported in Fig. 4. The first crystallization peak at Tx_1 = 504°C is shifted toward lower temperatures with increasing annealing time. After 23h of heat treatment, this peak vanishes indicating the whole crystallization of the associated phase. At this time, the main crystallization peak at Tx_2 = 545°C is still observable and is not really affected by the heat treatment. This peak is strongly reduced and shifted at 65h of heat treatment showing that a second crystalline phase appears in the matrix for longer annealing time.

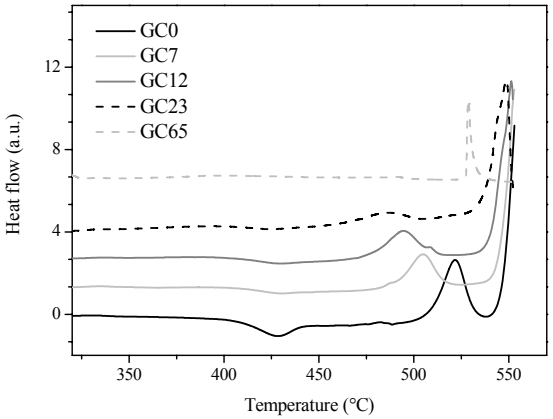

Fig. 4. DSC curves of the base glass GC0 and glass ceramics.

3.4 Structural analysis

The X-ray patterns on the base glass and the glass ceramics at different heat treatment time are presented in Fig. 5.

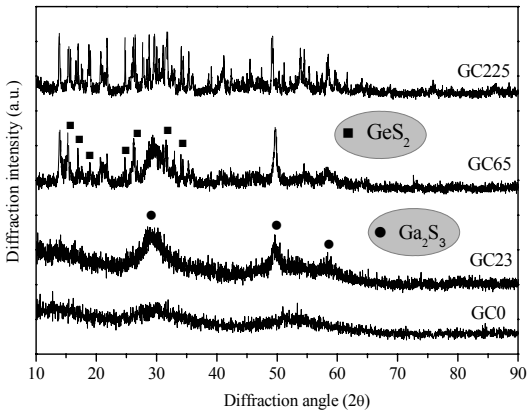

Fig. 5. X-ray diffraction of GC0, GC23, GC65 and GC225 glass ceramics.

The pattern of the parent glass GC0 confirms its glassy state. Some growing sharper peaks are observed in

the pattern of the GC23 sample. They can be correlated to the presence of crystals in the glassy matrix observed in Fig. 3 (b). The crystallization of this phase can also be associated to the first crystallization peak observed by DSC and which vanishes with increasing heat treatment time. Despite the low resolution of the X-ray patterns, the peak indexation reveals the formation of the α-Ga_2S_3 phase, as expected. Indeed, the network structure of such glasses is built up with [GeS_4] and [GaS_4] tetrahedral chains and complex $Cs^+[GaS_{3/2}Cl]^-$ structural units [26]. Then, regarding the high quantity of gallium introduced in this composition initially based on GeS_2 glass former, the nucleating role of Ga is not surprising.

Numerous sharper new peaks are observed in the diffraction pattern of the GC65 sample. As shown in Fig. 5, a good agreement is obtained with crystalline GeS_2. However the complete indexation of this pattern remains difficult from the existing crystallographic data. A sample was then heat treated 225h in order to help us in the identification of the crystallizing phases. While the indexation of the corresponding pattern (Fig. 5) is still ambiguous and complex, a relatively good agreement with some cesium based crystalline phases such as Cs_2S, Cs_2S_5, $CsGaS_x$ (x = 2, 3, 7) can be obtained.

The late crystallisation of germanium sulphide and cesium based phases can be correlated to the decrease of the highest crystallization peak observed in the DSC curves after long heat treatment time (Fig. 4), while the first peak at lower temperature which has almost vanished after 23h of annealing can be attributed to Ga_2S_3 crystalline phase.

By referring to these results, it can be assumed that the crystallisation of α-Ga_2S_3 which has a quite similar refractive index (~2.1) than the matrix limits the scatterings as reported by Hendy's equation [27] and permits to keep a good infrared transmission even with 50% of volumic crystallisation. Furthermore, the decrease of infrared transmission observed in Fig. 2 (b), due to scattering losses induced by crystals growth for annealing time higher than 23h, can be correlated with the crystallization of the whole glassy network associated to the strong decrease of the higher peak in the DSC curve (Fig. 4).

As mentioned above, the nucleation part is mainly observable in the 12 first hours of the annealing process, then nanocrystallites agglomerates to form aggregates of hundreds nm size. Also, the faster deterioration of the transmittance in the visible and near IR region (Fig. 2) can be explained by the growth of crystals which induce stronger scatterings.

3.5 Mechanical properties

The thermal dilatation coefficient α has been determined by TMA performed on the base glass and the GC23, GC36 and GC65 glass ceramics. The values, obtained with an accuracy of ± 0.2 K^{-1}, are reported in Table 1. The hardness (H_v) and the toughness (K_c) measured on the same samples using a Vickers micro indenter are also presented in Table 1.

Table 1. Dilatation coefficient, hardness and toughness of the base glass and glass ceramics.

Sample	α (.10^{-6} K^{-1})	H_v (kg.mm^{-2})	K_c (MPa.$mm^{1/2}$)
GC0	12.2	208	0.458
GC23	11.3	153	0.481
GC36	10.4	138.1	0.526
GC65	8.9	148.2	no cracks

A decrease of the dilatation coefficient is observed with increasing annealing time, leading to a relatively low value for GC36 and GC65 samples if compared with the base glass one and values generally reported with chalcogenide glasses (typically around 15.10^{-6} K^{-1}). Besides, an improvement of the toughness (K_c) of the glass ceramics is observed with annealing time. Firstly one can note that the measured toughness of the parent glass is twice higher in comparison with previous works carried out on selenide glasses [20]. Then the increased value measured for the GC36 sample reveals an improved resistance to fracture propagation of the material after heat treatment. With both decreasing thermal dilatation coefficient and increasing K_c, we can also attempt that its resistance to thermal shocks will be improved. Moreover, a decrease of hardness is observed between the base glass (H_v = 208 kg.mm^{-2}) and the glass ceramics one. The increasing toughness and decreasing hardness can be explained by a decrease of the network connectivity induced by the crystallization of the main coordinated atoms of the glassy matrix, Ge and Ga, resulting in a softer glassy matrix.

4. Conclusions

New transparent glass ceramics have been obtained in the Ga_2S_3 – GeS_2 – CsCl with appropriate heat treatment time and temperature. Crystals of typically 40 nm size have been reproducibly and homogeneously generated into the glassy matrix. The thermo-mechanical properties of the obtained glass ceramics have been improved in comparison with the parent glass ones and can be controlled according to the heat treatment time and temperature.

Contrarily to the first assumption made from the Ge-Sb-S-CsCl glassy system where cesium induces the beginning of crystallisation, CsCl do not play the role of nucleating agent in the Ge-Ga-S-CsCl vitreous system. In this case the crystallization is initiated with the formation of α-Ga_2S_3 crystals. Crystallization of GeS_2 and cesium based phases have also been observed for longer heat treatment. Further characterizations are under study in order to clearly understand the crystallization process in this material.

These new glass ceramics, with a broad band of transmittance and improved mechanical properties, present

a great interest for multi spectral imaging applications. In addition, their extended transmittance in the visible range in comparison with Ga_2S_3-GeS_2 glasses and the control of the ceramization process make them good candidates as rare earth ions hosts.

References

[1] A. Zakery, S. R. Elliott, J. Non-Cryst. Solids **330**, 1 (2003).
[2] K. Tanaka, J. Non-Cryst. Solids **352**, 2580 (2006).
[3] S. H. Messaddeq, V. R. Mastelaro, M. Siu Li, M. Tabackniks, D. Lezal, A. Ramos, Y. Messaddeq, App. Surf. Science **205**, 143 (2003).
[4] X. H. Zhang, B. Bureau, P. Lucas, C. Boussard-Pledel, J. Lucas, Chemistry - A European Journal **14**, 432 (2008).
[5] B. Bureau, J. L. Adam, Inorg. Chem. Highlights **2**, Wiley-VCH, 365 (2005).
[6] D. Le Coq, C. Boussard-Plédel, G. Fonteneau, T. Pain, B. Bureau, J. L. Adam, Mat. Res. Bull. **38**, 1745 (2003).
[7] J. S. Sanghera, I. D. Aggarwal, J. Non-Cryst. Solids **256-257**, 6 (1999).
[8] X. Zhang, H. Ma, J. Lucas, Y. Guimond, S. Kodjikian, J. Non-Cryst. Solids **336**, 49 (2004).
[9] S. Hocde, O. Loreal, O. Sire, C. Boussard-Pledel, B. Bureau, B. Turlin, J. Keirsse, P. Leroyer, J. Lucas, J. of Biomedical Optics **9**, 404 (2004).
[10] P. Lucas, D. Le Coq, C. Juncker, J. Collier, D. E. Boesewetter, C. Boussard-Pledel, B. Bureau, M. R. Riley, Appl. Spectrosc. **59**, 1 (2005).
[11] P. Lucas, M. R. Riley, C. Boussard-Plédel, B. Bureau, Analytical Biochemistry **351**, 1 (2006).
[12] C. Vigreux-Bercovici, E. Bonhomme, A. Pradel, J. E. Broquin, L. Labadie, P. Kern, Appl. Phys. Lett. **90**, 011110 (2007).
[13] P. Houizot, C. Boussard-Pledel, A. J. Faber, L. K. Cheng, B. Bureau, P. A. Van Nijnatten, W. L. M. Gielesen, J. Pereira do Carmo, J. Lucas, Opt. Express **15**, 12529 (2007).
[14] S. Kokenyesi, I. Ivan, M. Malyovanik, S. H. Messaddeq, Y. Messaddeq, S. J. L. Ribeiro, Physics and Chemistry of Glasses - European Journal of Glass Science and Technology Part B **47**, 211 (2006).
[15] X. Zhang, M. A. Hongli, J. Lucas, J. Non-Cryst. Solids **337**, 130 (2004).
[16] L. Calvez, H. L. Ma, J. Lucas, P. Glouannec, X. H. Zhang, J. Non-Cryst. Solids **353**, 4702 (2007).
[17] L. Calvez, H. L. Ma, J. Lucas, X. H. Zhang, J. Non-Cryst. Solids **354**, 1123 (2008).
[18] S. Z. Zhu, H. L. Ma, M. Matecki, X. H. Zhang, J. L. Adam, J. Lucas, J. Non-Cryst. Solids **351**, 3309 (2005).
[19] M. Hongli, L. Calvez, B. Bureau, M. Le Floch, X. Zhang, L. Jacques, J. Phys. Chem. of Solids **68**, 968 (2007).
[20] L. Calvez, H. L. Ma, J. Lucas, X. H. Zhang, Advanced Materials **19**, 129 (2007).
[21] V. Seznec, H. L. Ma, X. H. Zhang, V. Nazabal, J.-L. Adam, X. S. Qiao, X. P. Fan, Opt. Mater. **29**, 371 (2006).
[22] Y. Ledemi, L. Calvez, M. Rozé, X. H. Zhang, B. Bureau, M. Poulain, Y. Messaddeq, J. Opt. and Adv. Mater. **9**, 3751 (2007).
[23] D. K. Murray, J. W. Chang, J. F. Haw, Journal of the American Chemical Society **115**, 4732 (1993).
[24] J. Skibsted, T. Vosegaard, H. Bildsoe, H. J. Jakobsen, Journal of Physical Chemistry **100**, 14872 (1996).
[25] D. Massiot, F. Fayon, M. Capron, I. King, S. Le Calvé, B. Alonso, J.-O. Durand, B. Bujoli, Z. Gan, G. Hoatson, Magnetic Resonance in Chemistry **40**, 70 (2002).
[26] Y. S. Tver'yanovitch, E. G. Nedoshovenko, V. V. Aleksandrov, E. Y. Turkina, A. S. Tver'yanovitch, I. A. Sokolov, Glass Physics and Chemistry **22**, 9 (1996).
[27] S. Hendy, Appl. Phys. Lett. **81**, 1171 (2002).

*Corresponding author: yannickledemi@yahoo.fr